

# Grafting of Thiophenecarboxylates into Magnetic Transition Metal Hydroxide Layers

Aude Demessence,\* Guillaume Rogez, and Pierre Rabu\*

*Institut de Physique et Chimie des Matériaux de Strasbourg, UMR 7504 CNRS-ULP, 23, rue du Loess, BP 43, 67034 Strasbourg Cedex 2, France*

*Received February 14, 2006. Revised Manuscript Received April 13, 2006*

New hybrid organic/inorganic systems have been elaborated by insertion/grafting of thiophenecarboxylates into the layered transition metal hydroxides  $\text{Cu}_2(\text{OH})_3(\text{CH}_3\text{CO}_2)\cdot\text{H}_2\text{O}$  and  $\text{Co}_2(\text{OH})_3\text{NO}_3$ . The  $\text{Cu}_2(\text{OH})_{3.28}(\text{TA})_{0.72}\cdot 0.08\text{H}_2\text{O}$  (**1**;  $\text{TA}^-$ : 3-thiopheneacetate),  $\text{Cu}_2(\text{OH})_{3.04}(\text{TDC})_{0.48}\cdot 1.84\text{H}_2\text{O}$  (**3**;  $\text{TDC}^{2-}$ : 2,5-thiophenedicarboxylate),  $\text{Co}_2(\text{OH})_{3.38}(\text{TA})_{0.62}\cdot 1.52\text{H}_2\text{O}$  (**4**), and  $\text{Co}_2(\text{OH})_{3.44}(\text{TC})_{0.56}\cdot 0.7\text{H}_2\text{O}$  (**5**;  $\text{TC}^-$ : 2-thiophenecarboxylate) compounds have been synthesized by anionic exchange in alkaline media. Organic molecules interleaved between the layered inorganic framework are organized in a bilayer for the thiophenemonocarboxylates in Cu(II) and Co(II) materials and in a monolayer for the Cu(II) compound with the thiophenedicarboxylate. The insertion of the organic molecules into layered transition metal hydroxides modifies the magnetic properties of the inorganic layers, and ferromagnetic materials are obtained with Curie temperatures  $T_C$  up to 58 K and strong coercive fields up to 0.65 T.

## Introduction

Hetero-structured hybrids such as inorganic/inorganic, organic/inorganic (O/I)<sup>1,2</sup> and bio-/inorganic<sup>3</sup> systems have attracted considerable research interest because of their unusual physicochemical properties. The controlled packing of two molecular entities in the same material is suitable for providing new multifunctional systems. In these materials, each sub-network, organized at a nanoscale level, might exhibit its own properties or might contribute to new physical phenomena and novel applications. O/I compounds are an important trend in modern molecular and solid-state chemistry to design multi-functional materials, combining magnetism with optical activity,<sup>4,5</sup> nonlinear optical properties,<sup>6,7</sup> or conductivity.<sup>8</sup> However, these families of materials are generally characterized by weak intermolecular contacts which may be a limit for generating cooperative phenomena at relatively high temperatures. In this context, we developed another approach which consists of the combination by a strong connection of two sub-networks, one corresponding to transition metal ions coupled in an ionic-covalent way via hydroxo ligands and the other formed by molecules with a donor or acceptor  $\pi$  electron system. The inorganic sub-network can be magnetic; the organic molecules can

simultaneously have a structuring effect and bring an additional property such as conductivity, luminescence, or optical activity.

In this respect, the layered transition metal hydroxides,  $\text{M}_2(\text{OH})_3\text{X}$  ( $\text{M}(\text{II}) = \text{Co}, \text{Cu}, \text{Ni}, \text{Mn}$  and  $\text{X} = \text{NO}_3^-, \text{CH}_3\text{CO}_2^-, \text{Cl}^-$ ), with botallackite or brucite-type structures are appropriate for the design of new O/I materials.<sup>9–11</sup> Indeed, the presence of short metal–metal distances (ca. 0.3 nm) brought about by the  $\mu_3$  coordination mode of the  $\text{OH}^-$  moieties within the hydroxide layers results in efficient magnetic interactions by exchange coupling along the metal–oxygen–metal pathways, leading to a ferromagnetic, anti-ferromagnetic, or ferrimagnetic order. Moreover, the structure of these layered transition metal hydroxides can be tuned by the functionalization of the layers. The  $\text{X}^-$  anion located in the interlayer space may be substituted by a large variety of organic molecules via anionic exchange reaction.<sup>12</sup> Such interleaved species can be used as pillars or as connectors between the magnetic layers with a strong connection favoring a real interaction between the electronic populations of each sub-network<sup>11,13</sup> and can bring their own physical property.

Recently, luminescent oligo phenylene vinylene carboxylates have been inserted between magnetic Ni(II)-based hydroxide layers. In that hybrid compound, which is ferromagnetic below the Curie temperature  $T_C = 10$  K, it has been shown that the magnetic ordering may influence the

\* To whom correspondence should be addressed. Fax: (+33) 3-88-10-72-47. Tel.: (+33) 3-88-10-71-35 E-mail: aude.demesence@ipcms.u-strasbg.fr (A.D.), pierre.rabu@ipcms.u-strasbg.fr (P.R.).

- (1) Choy, J.-H.; Kwon, S.-J.; Park, G.-S. *Science* **1998**, *280*, 1589.
- (2) Sanchez, C.; Soler-Illia, G. J. d. A. A.; Ribot, F.; Lalot, T.; Mayer, C. R.; Cabuil, V. *Chem. Mater.* **2001**, *13*, 3061.
- (3) Choy, J.-H.; Kwak, S.-Y.; Park, J.-S.; Jeong, Y.-J.; Portier, J. J. *Am. Chem. Soc.* **1999**, *121*, 1399.
- (4) Minguet, M.; Luneau, D.; Lhotel, E.; Villar, V.; Paulsen, C.; Amabilino, D. B.; Veciana, J. *Angew. Chem., Int. Ed.* **2002**, *41*, 586.
- (5) Rikken, G. L.; Raupach, E. *Nature* **2000**, *405*, 932.
- (6) Lacroix, P. G.; Malfant, I.; Bénard, S.; Yu, P.; Rivière, E.; Nakatani, K. *Chem. Mater.* **2001**, *13*, 441.
- (7) Bénard, S.; Léaustic, A.; Rivière, E.; Yu, P.; Clément, R. *Chem. Mater.* **2001**, *13*, 3709.
- (8) Coronado, E.; Galan-Mascaros, J. R.; Gomez-Garcia, C. J.; Laukhin, V. *Nature* **2000**, *408*, 447.

- (9) Demessence, A.; Rogez, G.; Rabu, P. *Actual. Chim.* **2006**, 293, 17.
- (10) Taibi, M.; Ammar, S.; Jouini, N.; Fiévet, F.; Molinié, P.; Drillon, M. *J. Mater. Chem.* **2002**, *12*, 3238.
- (11) Rabu, P.; Drillon, M. *Adv. Eng. Mater.* **2003**, *5*, 189.
- (12) Rabu, P.; Drillon, M.; Awaga, K.; Fujita, W.; Sekine, T. In *Magnetism: Molecules to Materials*; Miller, J. S., Drillon, M., Eds.; Wiley-VCH: Weinheim, 2001; p 357.
- (13) Rabu, P.; Drillon, M. In *Handbook of Organic-Inorganic Hybrid Materials and Nanocomposites*; Nalwa, H. S., Ed.; American Scientific Publishers: Stevenson Ranch, 2003; Vol. 1, p 297.

luminescence of the inserted organic molecules.<sup>14</sup> Keeping up our aim to combine photoluminescence and/or conductivity with magnetism in the same materials, we have chosen to insert oligothiophenes<sup>15</sup> functionalized with carboxylates into layered transition metal hydroxides.

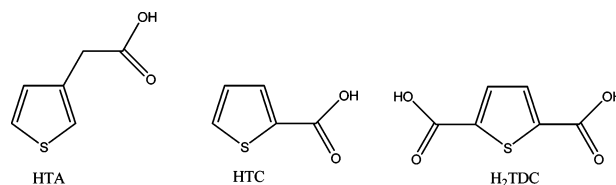
The monothiophenecarboxylates are particularly used in material sciences for their aromaticity. In the field of the luminescent materials, they are interesting because of their ability to absorb and to transfer efficiently the energy of the  $\pi$ ,  $\pi^*$  excited state to rare earth ions increasing their luminescence quantum yield.<sup>16–18</sup> Such energy transfer has been shown to induce a strong red light emission in lanthanide(III) complexes.<sup>19,20</sup>

Thiophenecarboxylates have been also extensively employed to obtain transition metal coordination complexes. For example, Byrnes et al. have reported intense metal-to-ligand charge transfer in complexes, in which 2-thiophenecarboxylate ( $\text{TC}^-$ ) or 2,5-thiophenedicarboxylate ( $\text{TDC}^{2-}$ ) are attached to dinuclear centers (Mo or W) having metal–metal quadruple bonds.<sup>21,22</sup> Many copper, zinc, cobalt, and manganese complexes mixing  $\text{H}_2\text{TDC}$  and nitrogen ligands were investigated.<sup>23,24</sup> Their crystal structures were solved, and some of their electrochemical properties were studied.<sup>25,26</sup> Moreover, coordination of thiopheneacetate to copper(II) with or without additional nitrogen ligand has been particularly investigated.<sup>27,28</sup>

However, even if complexes with thiophenecarboxylates are known, to the best of our knowledge only two magnetic studies have been reported, one on the copper(II) compound with thiodiglycolic acid and nitrogen ligands<sup>29</sup> and the other on the single-molecule magnet  $[\text{Mn}_{12}\text{O}_{12}(\text{O}_2\text{CC}_4\text{H}_3\text{S})_{16}(\text{H}_2\text{O})_4]$ .<sup>30</sup>

It is worth noticing also that thiophene rings are electron-rich  $\pi$ -systems and were used to stabilize the electron-attracting nitroxide radicals. Indeed, Iwamura et al. have

**Scheme 1. Employed Thiophenecarboxylic Acids: HTA (3-Thiopheneacetic Acid), HTC (2-Thiophenecarboxylic Acid), and  $\text{H}_2\text{TDC}$  (2,5-Thiophenedicarboxylic Acid)**



synthesized organic magnetic molecules by functionalizing a thiophene ring with two nitroxide radicals in the 2,4 or 2,5 positions. They demonstrated that magnetic interactions between the two radicals could occur through the thiophene ring because of spin polarization through the  $\pi$  system. The radicals can interact ferro- or antiferromagnetically depending on their relative position on the ring.<sup>31</sup> With respect to our interest of designing new multifunctional systems by the grafting of molecules into transition metal hydroxides, the thiophenecarboxylates appear very appealing, as a result of their luminescent properties and also because of the possibility they offer to tune the magnetic coupling between spin layers depending on the position of the carboxylate functions.

One example of insertion of  $\text{TC}^-$  between layered double hydroxides (LDH) was already reported. The electrochemical study was carried out, and the authors have shown that dimerization of the organic ligand occurs during the insertion of the monomeric counteranions in the confined space.<sup>32</sup> To demonstrate the validity of our approach, we describe here our first results on the grafting of monothiophenecarboxylates into layers of Cu(II) and Co(II) hydroxides.

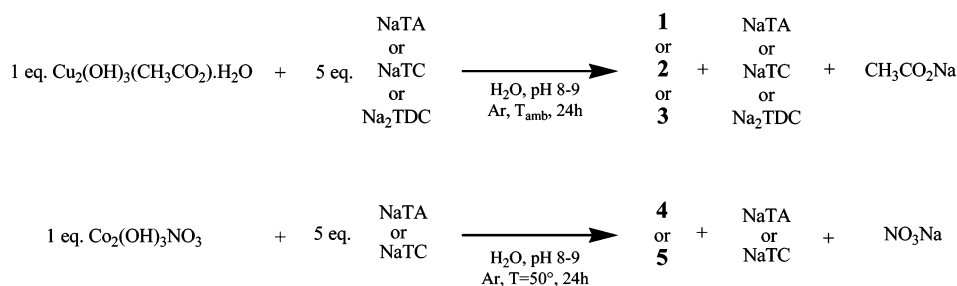
The purpose of this paper is to discuss the synthesis and structure–property correlations for this series of layered hybrid magnetic materials interleaved by three different monothiophenecarboxylates, namely, the hydroxide-based compounds of general formula:  $\text{M}_2(\text{OH})_{4-nx}(\text{A}^{n-})_x \cdot z\text{H}_2\text{O}$  with  $\text{M} = \text{Co}$  and  $\text{Cu}$  and  $\text{A} = \text{TA}^-$ ,  $\text{TC}^-$ , and  $\text{TDC}^{2-}$  (Scheme 1;  $\text{TA}^- = 3$ -thiopheneacetate).

## Results and Discussion

**Synthesis.** The compounds  $\text{Cu}_2(\text{OH})_{3.28}(\text{TA})_{0.72} \cdot 0.08\text{H}_2\text{O}$  (**1**),  $\text{Cu}_2(\text{OH})_{\sim 3.2}(\text{TC})_{\sim 0.8} \cdot \sim 0.1\text{H}_2\text{O}$  (**2**),  $\text{Cu}_2(\text{OH})_{3.04}(\text{TDC})_{0.48} \cdot 1.84\text{H}_2\text{O}$  (**3**),  $\text{Co}_2(\text{OH})_{3.38}(\text{TA})_{0.62} \cdot 1.52\text{H}_2\text{O}$  (**4**), and  $\text{Co}_2(\text{OH})_{3.44}(\text{TC})_{0.56} \cdot 0.7\text{H}_2\text{O}$  (**5**) have been prepared by anion-exchange reaction,<sup>33,34</sup> starting from  $\text{Cu}_2(\text{OH})_3(\text{CH}_3\text{CO}_2) \cdot \text{H}_2\text{O}$  or  $\text{Co}_2(\text{OH})_3(\text{NO}_3)$ , as described in Experimental Section. In a basic aqueous solution corresponding to an excess of thiophenecarboxylic acid sodium salt (for HTC,  $\text{pK}_a = 3.48$ ; for HTA,  $\text{pK}_a = 4.39$ ; and for  $\text{H}_2\text{TDC}$ ,  $\text{pK}_a = 3.18$  and 4.28),<sup>25,35</sup> the acetate or nitrate ions of the starting materials were exchanged with the thiophenecarboxylates ( $\text{TC}^-$ ,  $\text{TA}^-$ ,

- (14) Rueff, J.-M.; Nierengarten, J.-F.; Gilliot, P.; Demessence, A.; Cregut, O.; Drillon, M.; Rabu, P. *Chem. Mater.* **2004**, *16*, 2933.
- (15) Stott, T. L.; Wolf, M. O. *Coord. Chem. Rev.* **2003**, *246*, 89.
- (16) Teotonio, E. E. S.; Felinto, M. C. F. C.; Brito, H. F.; Malta, O. L.; Trindade, A. C.; Najjar, R.; Strek, W. *Inorg. Chim. Acta* **2004**, *357*, 451.
- (17) Yuan, L.; Li, Z.; Sun, J.; Zhang, K. *Spectrochim. Acta, Part A* **2003**, *59*, 2949.
- (18) Yuan, L.; Yin, M.; Yuan, E.; Sun, J.; Zhang, K. *Inorg. Chim. Acta* **2004**, *357*, 89.
- (19) Yin, M.-C.; Yuan, L.-J.; Ai, C.-C.; Wang, C.-W.; Yuan, E.-T.; Sun, J.-T. *Polyhedron* **2004**, *23*, 529.
- (20) Cai, L.-Z.; Chen, W.-T.; Wang, M.-S.; Guo, G.-C.; Huang, J.-S. *Inorg. Chem. Commun.* **2004**, *7*, 611.
- (21) Byrnes, M. J.; Chisholm, M. H. *Chem. Commun.* **2002**, 2040.
- (22) Byrnes, M. J.; Chisholm, M. H.; Clark, R. J. H.; Gallucci, J. C.; Hadad, C. M.; Patmore, N. J. *Inorg. Chem.* **2004**, *43*, 6334.
- (23) Sun, X.-Z.; Ye, B.-H. *Acta Crystallogr., Sect. E* **2004**, *E60*, m878.
- (24) Chen, B.-L.; Mok, K.-F.; Ng, S.-C.; Drew, M. G. B. *New J. Chem.* **1999**, *23*, 877.
- (25) Chen, B. L.; Mok, K. F.; Ng, S.-C.; Feng, Y.-L.; Liu, S.-X. *Polyhedron* **1998**, *17*, 4237.
- (26) Chen, B.-L.; Mok, K.-F.; Ng, S.-C.; Drew, M. G. B. *Polyhedron* **1999**, *18*, 1211.
- (27) Drożdżewski, P.; Brożyna, A.; Kubiak, M. *J. Mol. Struct.* **2004**, *707*, 131.
- (28) Marinho, M. V.; Yoshida, M. I.; Guedes, K. J.; Krambrock, K.; Bortoluzzi, A. J.; Horner, M.; Machado, F. C.; Teles, W. M. *Inorg. Chem.* **2004**, *43*, 1539.
- (29) Kopel, P.; Travnický, Z.; Marek, J.; Korabik, M.; Mrozinski, J. *Polyhedron* **2003**, *22*, 411.
- (30) Kuroda-Sowa, T.; Nogami, T.; Konaka, H.; Maekawa, M.; Munakata, M.; Miyasaka, H.; Yamashita, M. *Polyhedron* **2003**, *22*, 1795.

- (31) Mitsumori, T.; Inoue, K.; Koga, N.; Iwamura, H. *J. Am. Chem. Soc.* **1995**, *117*, 2467.
- (32) Tronto, J.; Sanchez, K. C.; Crepaldi, E. L.; Naal, Z.; Klein, S. I.; Valim, J. B. *J. Phys. Chem. Solids* **2004**, *65*, 493.
- (33) Vivani, R.; Masci, S.; Alberti, G. *Inorg. Chem.* **2004**, *43*, 368.
- (34) Meyn, M.; Beneke, K.; Lagaly, G. *Inorg. Chem.* **1993**, *32*, 1209.
- (35) *Handbook of Chemistry and Physics*, 64th ed.; CRC Press: Boca Raton, FL, 1983–1984.

**Scheme 2. Chemical Reactions To Graft Thiophenecarboxylates into Layered Transition Metal Hydroxides**

or TDC<sup>2-</sup>) according to Scheme 2. The chemical formulas have been established on the basis of the elemental analysis and scaled to two M(II) ions for direct comparison with the starting compounds (see Experimental Section). All the magnetic findings are consistent with the metal(II) contents as shown below. Attempts to synthesize by anionic exchange a hybrid compound with Co(II) and TDC<sup>2-</sup> were unsuccessful. Indeed two distinct phases are present in the final product, and by changing the experimental conditions, it was impossible to isolate one.

**Structure.** *Powder X-ray Structural Analyses.* All the compounds exhibit a lamellar structure as evidenced from their X-ray diffraction (XRD) patterns that show, in the low  $2\theta$  range, intense 00 $l$  diffraction lines, up to at least the third harmonic (Figures 1 and 2). This corresponds to the stacking periodicity of the hydroxide-based layers (basal spacing). During the exchange process, the completeness of the reaction is checked by the abrupt change in the peak positions, by comparison with the starting materials Cu<sub>2</sub>(OH)<sub>3</sub>(CH<sub>3</sub>CO<sub>2</sub>)·H<sub>2</sub>O ( $d_{00l}$  = 0.93 nm) or Co<sub>2</sub>(OH)<sub>3</sub>(NO<sub>3</sub>) ( $d_{00l}$  = 0.69 nm). For the copper(II) monocarboxylate compounds, the experimental basal spacing is 1.59 nm for **1** and 1.45 nm for **2**. As shown for the series of parent compounds Cu(OH)<sub>4- $n$ x</sub>(A <sup>$n-$</sup> ) <sub>$x$</sub> · $z$ H<sub>2</sub>O (A = CH<sub>3</sub>-(CH<sub>2</sub>) <sub>$n$</sub> -CO<sub>2</sub>),<sup>36,37</sup> the products **1** and **2** are expected to exhibit hydroxide-based layers consisting of a quasi-planar triangular array of copper(II) ions in an octahedral surrounding. Comparisons of the XRD patterns with that of the parent copper hydroxide acetate shows similarities in the range 30–45°, which is attributed to  $hk0$  (in-plane) peaks. In particular, it is worth noticing the occurrence of a line at 0.27 nm for all the copper compounds, which corresponds well to the 120 line of the starting material. This suggests that the structure within the layers does not vary much. Actually, such variation is essentially due to the necessary adaptation of the molecular area of each metal ion to the molecular area of the grafted anions. More precise analysis would be necessary for a full pattern indexing, but it was not possible here because of large and superimposed diffraction peaks. According to the density functional theory calculations carried out by Tsuzuki et al.<sup>38</sup> to establish the origin of the  $\pi$ -stacking in thiophene dimers, thiophene rings of adjacent layers should adopt the preferential T conformation as a result of the strong Coulombic interaction between the hydrogen on the carbon in position

**5** and the negatively charged carbon of another thiophene, as it occurs in the thiophenecarboxylic acid (Scheme 3).<sup>39,40</sup> The structure of the latter consists of the stacking of hydrogen bonded TC acid forming layers with an interlayer space between the perpendicular thiophene rings of approximately 0.19 nm along the  $c$  axis (with a tilt angle of the thiophenes of 50° with respect to this  $c$  axis).

On this basis and taking into account the length of the grafted species (0.55 nm for TA and 0.47 nm for TC), the interlayer distances in **1** and **2** are consistent with an arrangement of the organic molecules in bilayers between the hydroxide sheets, the thickness of which is estimated to be ~0.3 nm.<sup>36</sup> Note that dimerization of thiophenecarboxylates in the confined space is ruled out, contrary to what is observed in LDH,<sup>32</sup> because the interlamellar distance is too large. (Indeed, the grafting of 2,2'-bithiophene-5,5'-dicarboxylic acids between hydroxide copper layers, recently carried out in our laboratory, results in an interlamellar distance of 1.29 nm compared to 1.45 nm for **2**.) The suggested structural models, where the adjacent thiophene rings are in a T conformation, are presented in Scheme 4. In the case of compound **2**, an additional peak at 2.05 nm is observed in the diffraction pattern, indicating the presence of another exchange product, possibly corresponding to a staggering phenomenon<sup>41</sup> or to a different conformation of the thiophenecarboxylates. Nevertheless, it is difficult to conclude because no related harmonic appears in this pattern. Varying the synthesis conditions leads to different intensity ratios between this peak and the 00 $l$  harmonics; however, it was always present with significant intensity. Accordingly, precise and consistent formulation of this compound was also difficult. In the case of compound **3**, which has a basal spacing of 1.16 nm with a thiophenedicarboxylate length of 0.79 nm, it appears that the ligand TDC is bridging quasi perpendicularly adjacent inorganic layers, like in terephthalate<sup>42</sup> and alkanedioate<sup>43</sup> analogues. Figure 3 shows a scanning electron microscopy (SEM) photo of compound **3**, which is typical of all these hybrid materials that are obtained as thin platelet shaped microcrystals in agreement with the lamellar character of their structure.

(36) Laget, V.; Hornick, C.; Rabu, P.; Drillon, M. *J. Mater. Chem.* **1999**, 9, 169.

(37) Fujita, W.; Awaga, K.; Yokoyama, T. *Inorg. Chem.* **1997**, 36, 196.

(38) Tsuzuki, S.; Honda, K.; Azumi, R. *J. Am. Chem. Soc.* **2002**, 124, 12200.

(39) Roux, M. V.; Temprado, M.; Jiménez, P.; Davalos, J. Z.; Foces-Foces, C.; Garcia, M. V.; Redondo, M. I. *Thermochim. Acta* **2003**, 404, 235.

(40) Nardelli, M.; Fava, G.; Giraldo, G. *Acta Crystallogr.* **1962**, 15, 737.

(41) Pisson, J.; Taviot-Guého, C.; Israël, Y.; Leroux, F.; Munsch, P.; Itié, J.-P.; Briois, V.; Morel-Desrosiers, N.; Besse, J.-P. *J. Phys. Chem. B* **2003**, 107, 9243.

(42) Abdelouhab, S.; François, M.; Elkaim, E.; Rabu, P. *Solid State Sci.* **2005**, 7, 227.

(43) Rabu, P.; Rueff, J.-M.; Huang, Z.-L.; Angelov, S.; Souletie, J.; Drillon, M. *Polyhedron* **2001**, 20, 1677.



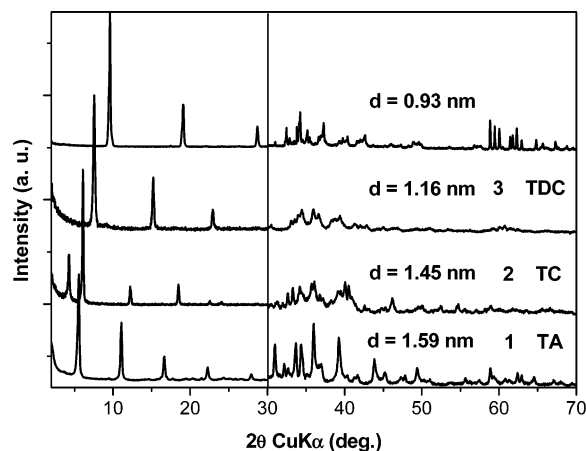


**Figure 1.** Powder XRD patterns of  $\text{Cu}_2(\text{OH})_3(\text{CH}_3\text{CO}_2)\cdot\text{H}_2\text{O}$  (upper curve) and compounds  $\text{Cu}_2(\text{OH})_{3.28}(\text{TA})_{0.72}\cdot 0.08\text{H}_2\text{O}$  (1),  $\text{Cu}_2(\text{OH})_{\sim 3.2}(\text{TC})_{\sim 0.8}\cdot \sim 0.1\text{H}_2\text{O}$  (2), and  $\text{Cu}_2(\text{OH})_{3.04}(\text{TDC})_{0.48}\cdot 1.84\text{H}_2\text{O}$  (3) showing the shift of 00l diffraction lines. The 30–70° range is zoomed in to highlight the peaks in this region.

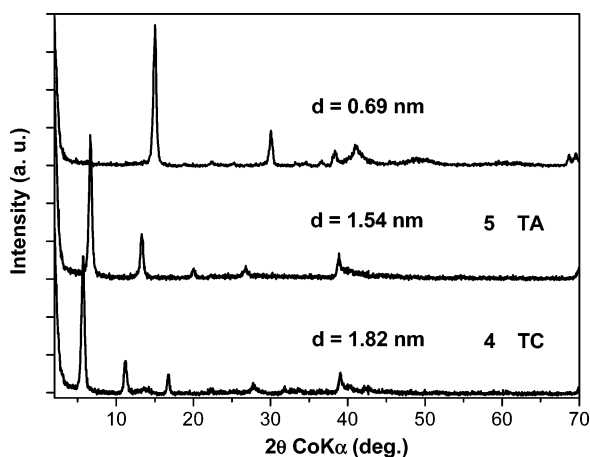
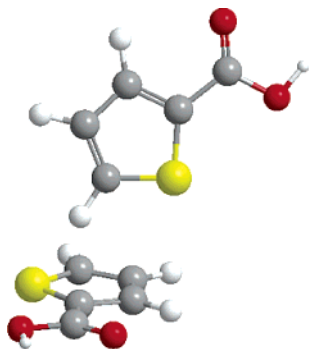


**Figure 2.** Powder XRD patterns of  $\text{Co}_2(\text{OH})_3\text{NO}_3$  (upper curve)  $\text{Co}_2(\text{OH})_{3.38}(\text{TA})_{0.62}\cdot 1.52\text{H}_2\text{O}$  (4), and  $\text{Co}_2(\text{OH})_{3.44}(\text{TC})_{0.56}\cdot 0.7\text{H}_2\text{O}$  (5) showing the shift of 00l diffraction lines.

### Scheme 3. Preferential T Conformation between Two Thiophene Rings



The cobalt(II) compounds **4** and **5** are characterized by a basal spacing larger than that of the copper(II) analogue by 0.23 nm for **4**, with a distance of 1.82 nm, and by 0.09 nm for **5**, with a distance of 1.54 nm (Figure 2). Such a difference is explained by an increase of the thickness of the inorganic layer. As already emphasized for the alkylcarboxylate,<sup>36,44</sup>

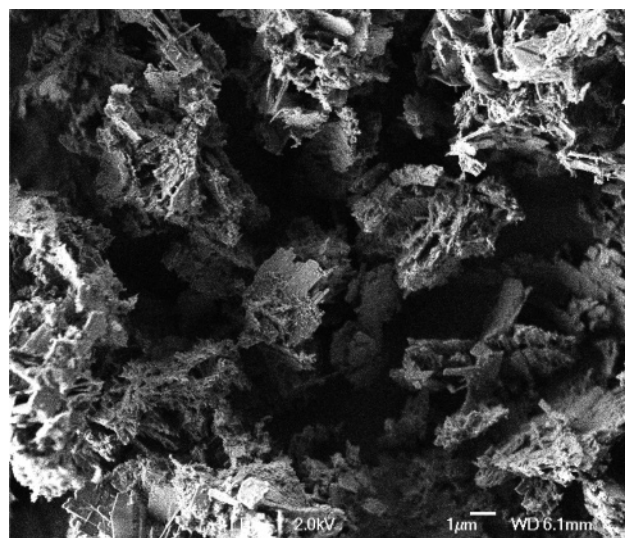


**Figure 3.** SEM image of compound **3**.

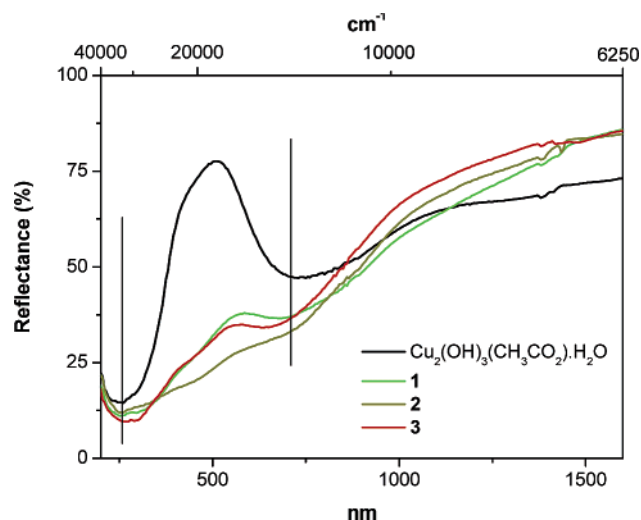


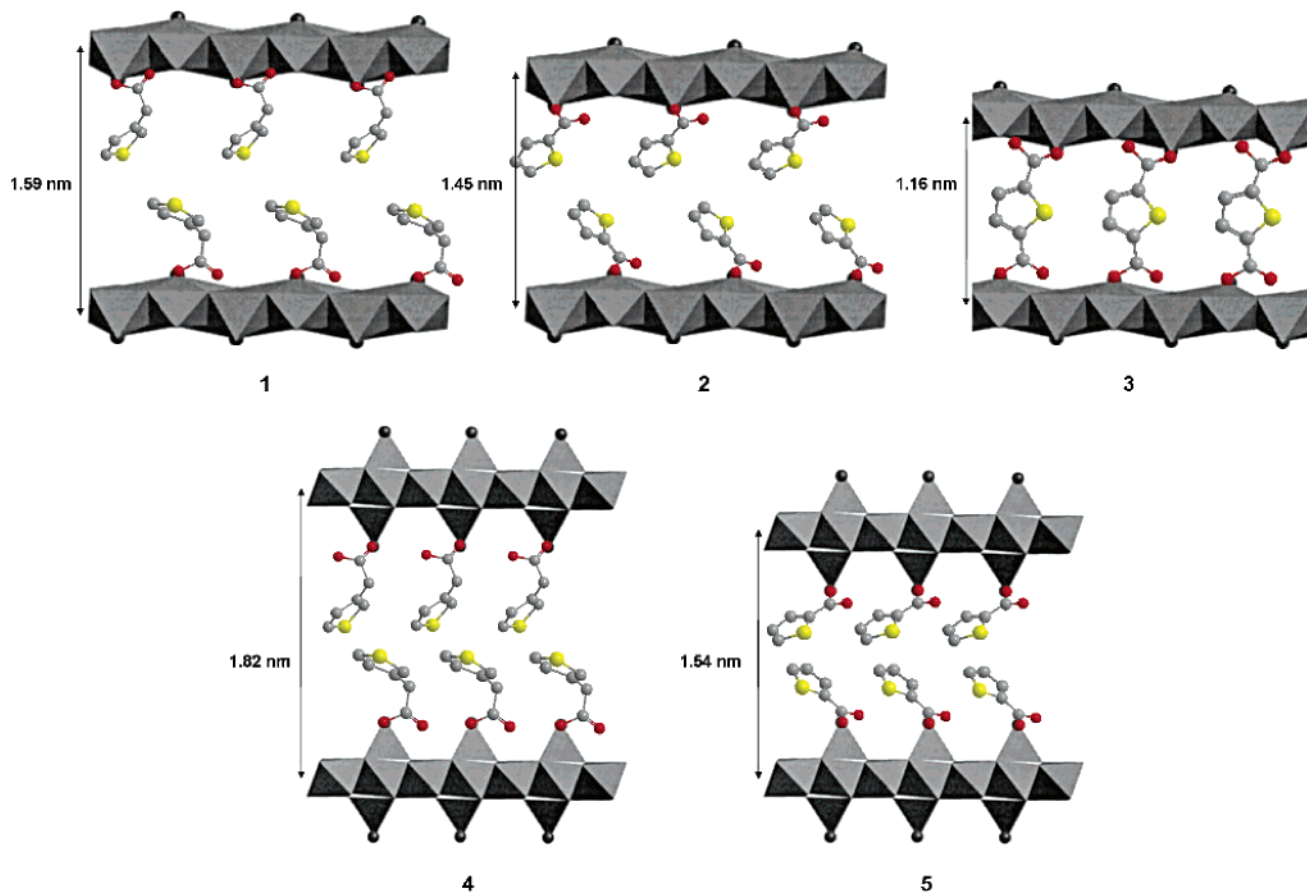
**Figure 4.** UV-vis reflectance spectra of compounds  $\text{Cu}_2(\text{OH})_{3.28}(\text{TA})_{0.72}\cdot 0.08\text{H}_2\text{O}$  (1; green),  $\text{Cu}_2(\text{OH})_{\sim 3.2}(\text{TC})_{\sim 0.8}\cdot \sim 0.1\text{H}_2\text{O}$  (2; dark yellow), and  $\text{Cu}_2(\text{OH})_{3.04}(\text{TDC})_{0.48}\cdot 1.84\text{H}_2\text{O}$  (3; red) compared to the starting material  $\text{Cu}_2(\text{OH})_3(\text{CH}_3\text{CO}_2)\cdot\text{H}_2\text{O}$  (black).

exchange reactions in the Co(II) hydroxide systems modify the structure of the metal-based layers, with the occurrence of tetrahedral sites on both sides of the initial octahedral monolayer forming triple-deck sheets as in the model compound  $\text{Zn}_5(\text{OH})_8(\text{NO}_3)_2\cdot 2\text{H}_2\text{O}$ .<sup>45</sup> In this kind of layered structure, it is generally assumed that each carboxylate function is linked to one cobalt ion in a tetrahedral environment. So the number of TA or TC ligands corresponds to the number of tetrahedral cobalt ions. From the chemical formulation the octahedral to tetrahedral cobalt ion ratio is deduced to be  $\sim 69:31$  for **4** and  $\sim 72:28$  for **5**. The magnetic measurements are in good agreement with these results (see Magnetic Properties). For an inorganic layer thickness established to about 0.73 nm, the thiophenecarboxylates are tilted (35 and 49° with respect to the *c* axis for **4** and **5**, respectively) and arranged in a bilayer, probably with the preferential T conformation between the thiophene rings as shown in Scheme 4. It is worth noticing that compared to the starting cobalt hydroxide nitrate the XRD pattern exhibits

(44) Laget, V.; Hornick, C.; Rabu, P.; Drillon, M.; Ziessel, R. *Coord. Chem. Rev.* **1998**, *10*, 1024. Laget, V. Ph.D. Thesis, Université Louis Pasteur, Strasbourg, France, 1998.

(45) Stählin, W.; Oswald, H. R. *Acta Crystallogr., Sect. B* **1970**, *26*, 860.

**Scheme 4. Schematic Illustrations of the Proposed Structures of Compounds  $\text{Cu}_2(\text{OH})_{3.28}(\text{TA})_{0.72} \cdot 0.08\text{H}_2\text{O}$  (1),  $\text{Cu}_2(\text{OH})_{3.2}(\text{TC})_{0.8} \cdot 0.1\text{H}_2\text{O}$  (2), and  $\text{Cu}_2(\text{OH})_{3.04}(\text{TDC})_{0.48} \cdot 1.84\text{H}_2\text{O}$  (3) Based on the  $\text{Cu}_2(\text{OH})_3\text{NO}_3$  Structure and  $\text{Co}_2(\text{OH})_{3.38}(\text{TA})_{0.62} \cdot 1.52\text{H}_2\text{O}$  (4) and  $\text{Co}_2(\text{OH})_{3.44}(\text{TC})_{0.56} \cdot 0.7\text{H}_2\text{O}$  (5) Based on the  $\text{Zn}_5(\text{OH})_8(\text{NO}_3)_2 \cdot 2\text{H}_2\text{O}$  Structure**



similar features in the region of in-plane diffraction lines indicating turbostratic disorder like in the green parent,  $\text{Co}_7(\text{OH})_{12}(\text{NO}_3)_2 \cdot 3\text{H}_2\text{O}$ .<sup>46</sup>

**UV–Vis Reflectance Structural Studies.** The UV spectra of the copper compounds show the three characteristic bands of copper(II) carboxylate system (Figure 4).<sup>47</sup> The most intense absorption is observed in the range of 250–260 nm and corresponds undoubtedly to charge transfer ( $\text{O} \rightarrow \text{Cu}$ ). The second absorption band is observed between 370 and 385 nm as a shoulder, and the third appears between 665 and 740 nm. The bluish-green color of the cobalt(II) compounds is consistent with both tetrahedral and octahedral metallic coordinations, in contrast with the pink color of  $\text{Co}_2(\text{OH})_3(\text{NO}_3)$ , which exhibits only octahedral sites. The UV–vis reflectance spectra of compounds **4** and **5** are consistent with such metallic environments (Figure 5). The two UV–vis. spectra show five electronic transitions that are indeed characteristic of  $d^7$  metal ions in both octahedral and tetrahedral sites (see Experimental Section). The  $D_q$  values for octahedral (Oh) sites, for compounds **4** and **5**, are 890 and 880  $\text{cm}^{-1}$ , respectively, and Racah's parameters are  $B \approx 900$  and 890  $\text{cm}^{-1}$ , as evaluated from the observed transitions, which agree with a weak crystal field ( $D_q/B \approx 1$ ) and a high-spin configuration for the metal centers.<sup>47</sup> For

Td sites the parameters are  $D_q \approx 380$  and 370  $\text{cm}^{-1}$  for products **4** and **5**, respectively, and  $B \approx 730$   $\text{cm}^{-1}$  for the two compounds. Moreover, the magnetic behavior of these cobalt compounds regarding the saturation magnetization denotes the presence of Td and Oh sites (see magnetic part).

**Infrared Spectroscopic Properties.** The structure of the exchanged compounds was also investigated by Fourier transform infrared (FT-IR) spectroscopy (Figure 6). The presence of a broad feature in the hydroxyl stretching region (3000–3600  $\text{cm}^{-1}$ ) corresponds to the lattice water, according to the chemical analyses. The vibrations of the carboxylate group are well characterized by infrared spectroscopy. For the free acid ligands (not shown here) the spectra show a strong antisymmetrical vibration band  $\nu_{\text{as}}(\text{C}=\text{O})$  of COOH at 1700  $\text{cm}^{-1}$ . After deprotonation and coordination to a metal ion, this band is shifted in the 1545–1575  $\text{cm}^{-1}$  region, whereas the symmetrical vibration,  $\nu_{\text{s}}(\text{C}-\text{O})$ , is still observed in the 1370–1385  $\text{cm}^{-1}$  region (Table 1). Furthermore, the compounds **1**, **3**, and **4** exhibit a difference  $\Delta\nu$ , between  $\nu_{\text{as}}(\text{C}=\text{O})$  and  $\nu_{\text{s}}(\text{C}-\text{O})$ , of 170, 175, and 160  $\text{cm}^{-1}$ , respectively. The values are similar to those observed for the sodium salts ( $\Delta\nu = 170$   $\text{cm}^{-1}$  for NaTA and  $\Delta\nu = 177$   $\text{cm}^{-1}$  for Na<sub>2</sub>TDC), which suggest that the carboxylate groups are coordinated to metal ions in a bidentate bridging mode.<sup>48,49</sup> For comparison, Drożdżewski et al. have solved the crystal

(46) Laget, V.; Rouba, S.; Rabu, P.; Hornick, C.; Drillon, M. *J. Magn. Magn. Mater.* **1996**, 154, L7.

(47) Lever, A. B. P. *Inorganic Electronic Spectroscopy*, 2nd ed.; Elsevier: Amsterdam, 1984.

(48) Nakamoto, K. *Infrared and Raman Spectra of Inorganic and Coordination Compounds*; Wiley: New York, 1986.

(49) Deacon, G. B.; Phillips, R. J. *Coord. Chem. Rev.* **1980**, 33, 227.

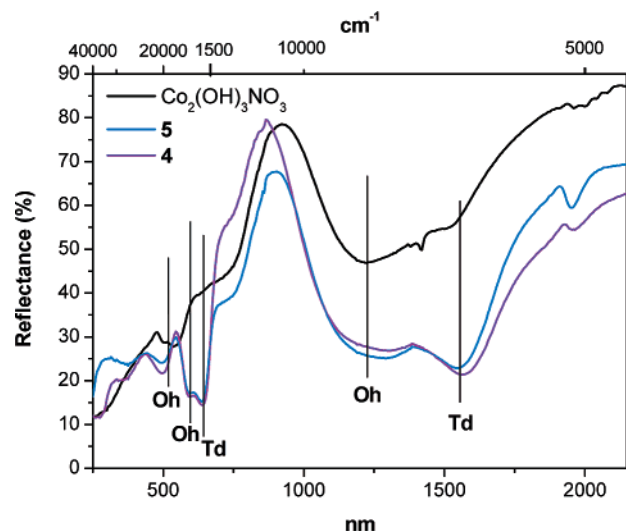


**Figure 5.** UV-vis reflectance spectra of compound  $\text{Co}_2(\text{OH})_{3.38}(\text{TA})_{0.62} \cdot 1.52\text{H}_2\text{O}$  (4; purple) and  $\text{Co}_2(\text{OH})_{3.44}(\text{TC})_{0.56} \cdot 0.7\text{H}_2\text{O}$  (5; blue) compared to the starting material  $\text{Co}_2(\text{OH})_3\text{NO}_3$  (black).

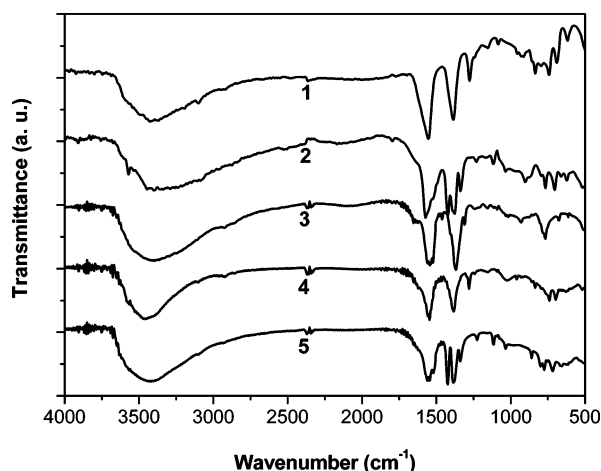


**Figure 6.** IR spectra for 1–5 compounds respectively from top to bottom.

**Table 1. Vibration Modes in Infrared Spectroscopy of the Carboxylate Functions in the Hybrid Materials**

	$\nu_{\text{as}}(\text{C}=\text{O})$ ( $\text{cm}^{-1}$ )	$\nu_{\text{s}}(\text{C}-\text{O})$ ( $\text{cm}^{-1}$ )	$\Delta\nu$ ( $\text{cm}^{-1}$ )
1	1555	1385	170
2	1575	1375	200
3	1545	1370	175
4	1545	1385	160
5	1555	1385	170

structure of a polymeric copper(II) complex with 2-TA,<sup>50</sup> and the infrared spectroscopy features are similar to those of **1**. The crystal structure of the manganese and TDC complex was solved, and a similar value of  $\Delta\nu$  was observed for a tetradentate bridging mode.<sup>24</sup> In the infrared spectra of compounds **2** and **5**, with the TC ligand, three bands appear in the 1575–1370  $\text{cm}^{-1}$  regions. Two bands are assigned to the  $\nu_{\text{as}}(\text{C}=\text{O})$  and  $\nu_{\text{s}}(\text{C}-\text{O})$  vibrational modes with  $\Delta\nu$  separations of 200 and 170  $\text{cm}^{-1}$  for compounds **2** and **5**, respectively. The  $\Delta\nu$  separation of 200  $\text{cm}^{-1}$  for compound **2** is between the  $\Delta\nu$  value expected for a monodentate coordination mode ( $\Delta\nu > 200 \text{ cm}^{-1}$ ) and the bridging bidentate coordination mode ( $\Delta\nu < 200 \text{ cm}^{-1}$ ). The presence of hydrogen bonds between oxygen atoms of carboxylates

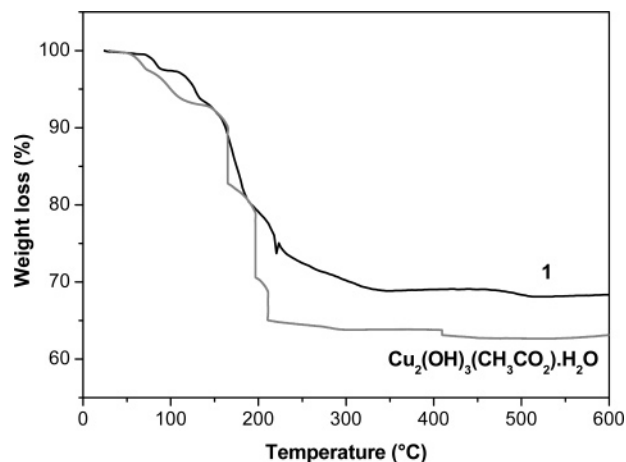


**Figure 7.** TGA curves for compound **1** compared to the starting material  $\text{Cu}_2(\text{OH})_3(\text{CH}_3\text{CO}_2) \cdot \text{H}_2\text{O}$ .

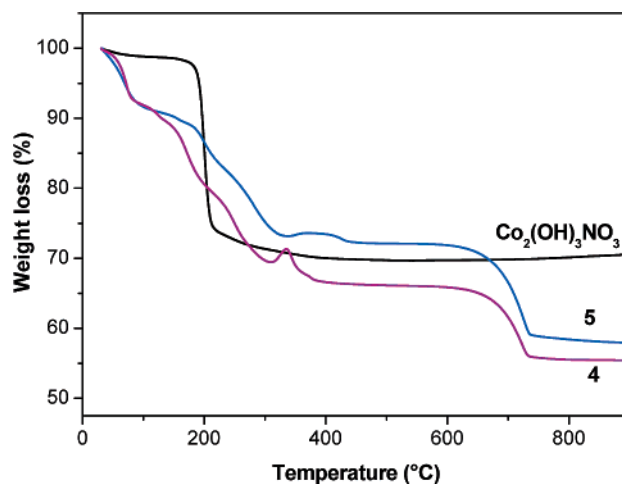


**Figure 8.** TGA curves for compounds **4** (purple) and **5** (blue) compared to the starting material  $\text{Co}_2(\text{OH})_3\text{NO}_3$  (black).

and hydrogen atoms of water or neighboring hydroxide can explain this high separation. The  $\Delta\nu$  separation for compound **5** is 170  $\text{cm}^{-1}$ , indicating that the TC ligand could be coordinated to the metal(II) in both the chelating and the bridging mode via the oxygen atoms of the carboxylic groups. Such bidentate–chelate coordination was seen in the crystal structure of  $\text{Eu}(\text{TC})_3(\text{H}_2\text{O})_3 \cdot 0.5\text{H}_2\text{O}$ .<sup>18</sup> IR spectra of compounds **2** and **5** exhibit also a very strong band at 1425  $\text{cm}^{-1}$  and a smaller at 1340  $\text{cm}^{-1}$ . These bands are present in the starting ligand (in acid and salt forms) and were assigned to a stretching vibration of the alkene moiety of the thiophene rings.<sup>51</sup> These bands are absent in the two differently substituted thiophenes, TA and TDC.

**Thermogravimetric Analysis (TGA).** Figures 7 and 8 show the TGA curves obtained in air with a heating rate of 2  $^\circ\text{C} \cdot \text{min}^{-1}$  for the copper compounds **1** and  $\text{Cu}_2(\text{OH})_3(\text{CH}_3\text{CO}_2) \cdot \text{H}_2\text{O}$ , of 0.5  $^\circ\text{C} \cdot \text{min}^{-1}$  for **3**, and of 5  $^\circ\text{C} \cdot \text{min}^{-1}$  for the cobalt compounds. A very low heating rate was applied for the copper materials because the last step in the decomposition is fast and very exothermic. However, the TGA curve for compound **3** is not given because of a strong exothermic combustion at 245  $^\circ\text{C}$  which is accompanied by a projection

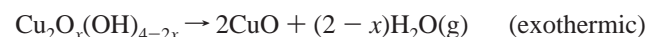
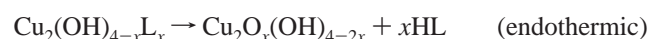
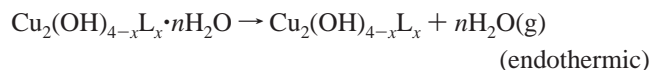
(50) Drożdżewski, P.; Brożyna, A.; Kubiak, M. *Polyhedron* **2004**, 23, 1785.

(51) Kwiatkowski, J. S.; Leszczynski, J.; Teca, I. *J. Mol. Struct.* **1997**, 436–437, 451.



of the solid out of the crucible even for low heating rate. The final thermal decomposition products, CuO and Co<sub>2</sub>O<sub>3</sub>, obtained at high temperature, were identified by powder XRD.

The results of TGA for compound **1** in comparison with the Cu<sub>2</sub>(OH)<sub>3</sub>(CH<sub>3</sub>CO<sub>2</sub>)·H<sub>2</sub>O<sup>52</sup> are presented in Figure 7. The copper hydroxide-based compounds exhibit a three step decomposition:



The first endothermic event corresponds to the loss of the water molecules of the interlayer region. The other events are poorly resolved and correspond to the complete thermal decomposition, which can be best represented by the two last reactions above. Compound **1** is characterized by a gradual weight loss of 5.5% (calcd, 0.5%) up to about 93 °C. The formation of the copper oxide is accompanied by an exothermic peak at 323 °C. The percentage of copper deduced from the weight loss at 500 °C is 45.1% (calcd, 45.3%). The compounds with cobalt ions are compared to the starting material Co<sub>2</sub>(OH)<sub>3</sub>NO<sub>3</sub><sup>53</sup> in Figure 8. The two hybrid compounds show three graduated and distinct weight losses. The first event is the elimination of the water molecules up to about 140 °C, 10.4% (calcd, 9.4%) for **4** and 9.5% (calcd, 4.8%) for **5**. The second weight loss of 22.8% up to ca. 400 °C and 18.3% up to ca. 450 °C accompanied by an exothermic peak on the Thermogravimetric Analysis (TGA) curve at 253 °C and 277 °C for, respectively, **4** and **5** can be assigned to the elimination of thiopheneacetic acid and thiophenecarboxylic acid followed by oxidation of divalent cobalt. The final weight loss at 700 °C is known to be related to the modification of the amorphous compound into cobalt oxide Co<sub>3</sub>O<sub>4</sub>.<sup>54</sup> The quantified cobalt is 40.8% (calcd, 40.6%) for **4** and 42.5% (calcd, 45.3%) for **5**. Summarizing, the insertion of the organic molecules does not modify significantly the thermal stability of the hybrid hydroxide-based materials compared to the starting materials.

**Photoluminescence Studies.** In contrast to their corresponding acids, which show weak fluorescence in the solid state, no emission was observed for the thiophenecarboxylate sodium salts. Similarly, they do not emit when they are grafted between the layers. According to the literature, pure thiophenes show a weak phosphorescence.<sup>55–58</sup> It is also known that the photoluminescence quantum yield (PLQY)

of polythiophenes decreases in the solid state compared to the solution, as a result of a quenching occurring when the thiophene rings are  $\pi$ -stacked.<sup>59</sup> The emission property is thus influenced by the aggregation. It was shown that when the molecules are parallel and placed at a distance of less than 0.5 nm, a complete quenching of photoluminescence occurs (shorter distance leads to excimer formation), while over 0.7 nm strongly reduced quenching is observed. It is worth noticing that for polythiophenes substituted with alkyl chains, the PLQY is higher in the solid state, because the arrangement of conjugated residues is un-faced; so the disorder favors the PL efficiency.<sup>60</sup> The lack of fluorescence for compounds **1–5** can be due to a  $\pi$ -stacking between the grafted thiophenecarboxylates, because of their repartition in the layers. The distances between the thiophene rings vary from 0.58 to 0.85 nm for the copper hybrids and from 0.54 to 0.93 nm for the cobalt compounds. (This repartition of thiophenes has been evaluated from the molecular area of metal ions deduced from the known structure of copper hydroxide acetate,<sup>52</sup> combined to the formulation of the hybrid materials.) Significant quenching may also be due to absorption by the inorganic networks followed by a non-radiative de-excitation.

**Magnetic Properties.** The variation of the interlamellar distance and the structure modification induced within the inorganic layers by the grafting of the exchange anions play an important role on the magnetic properties of the lamellar hydroxides. It was observed in previous work that for an interlamellar distance shorter than 1 nm these materials present a three-dimensional antiferromagnetic behavior at low temperature due to the exchange coupling (in the sense of orbital overlap) between the layers.<sup>12</sup> Indeed, the starting materials, that is, the copper hydroxy acetate and the cobalt hydroxy nitrate, exhibit both ferromagnetic layers which are coupled antiferromagnetically, with Neel temperatures  $T_N$  of 12 and 9 K, respectively. The insertion of organic entities between the magnetic layers of cobalt and copper hydroxide implies an increase of the distance between these layers, which cancels practically the exchange coupling above 1 nm. The hybrid materials can then order ferromagnetically as a result of efficient dipolar interactions between the ferromagnetic spins layers.<sup>61</sup> This coupling may be tuned by spin polarization along unsaturated bridging ligands.<sup>62</sup>

Temperature variation of the magnetic susceptibility,  $\chi$ , was measured using a SQUID magnetometer between 295 and 1.8 K under a magnetic field of 0.05 T. The  $\chi T = f(T)$  curves for the hybrid Cu-based hydroxides and the starting material are presented in Figure 9. Compound **1** exhibits a two-dimensional antiferromagnetic behavior over the whole temperature range, as illustrated by the continuous decay of the  $\chi T$  product from 0.82 emu·K·mol<sup>-1</sup> at 295 K to 0.05 emu·K·mol<sup>-1</sup> at 2 K. The inverse susceptibility (not shown) varies linearly with the temperature in the high-temperature

(52) Masciocchi, N.; Corradi, E.; Sironi, A.; Moretti, G.; Minelli, G.; Porta, P. *J. Solid State Chem.* **1997**, *131*, 252.

(53) Rabu, P.; Angelov, S.; Legoll, P.; Belaiche, M.; Drillon, M. *Inorg. Chem.* **1993**, *32*, 2463.

(54) Markov, L.; Petkov, K.; Petkov, V. *Thermochim. Acta* **1986**, *106*, 283.

(55) Flicker, W. M.; Mosher, O. A.; Kuppermann, A. *Chem. Phys. Lett.* **1976**, *38*, 489.

(56) Van Veen, E. H. *Chem. Phys. Lett.* **1976**, *41*, 535.

(57) Becker, R. S.; Seixas de Melo, J.; Maçanita, A. L.; Elisei, F. *J. Phys. Chem.* **1996**, *100*, 18683.

(58) Wan, J.; Hada, M.; Ehara, M.; Nakatsuji, H. *J. Chem. Phys.* **2001**, *114*, 842.

(59) Antolini, L.; Tedesco, E.; Barbarella, G.; Favaretto, L.; Sotgiu, G.; Zambianchi, M.; Casarini, D.; Gigli, G.; Cingolani, R. *J. Am. Chem. Soc.* **2000**, *122*, 9006.

(60) Destri, S.; Pasini, M.; Giovanella, U.; Porzio, W. *Mater. Sci. Eng., C* **2003**, *23*, 291.

(61) Drillon, M.; Panissod, P. *J. Magn. Magn. Mater.* **1998**, *188*, 93.

(62) Hornick, C.; Rabu, P.; Drillon, M. *Polyhedron* **2000**, *19*, 259.

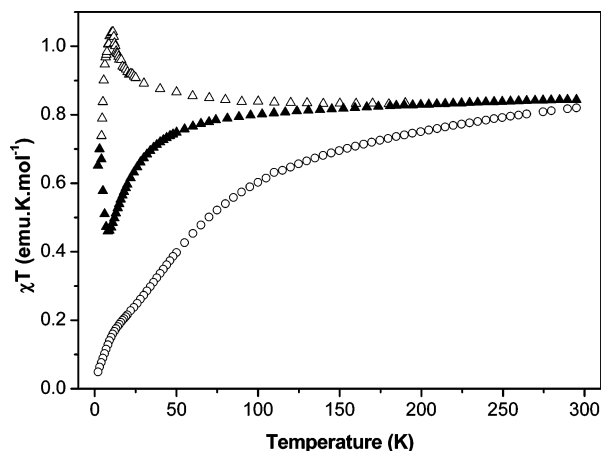


**Figure 9.** Magnetic behavior as  $\chi T$  vs  $T$  plots of compounds  $\text{Cu}_2(\text{OH})_{3.28}(\text{TA})_{0.72} \cdot 0.08\text{H}_2\text{O}$  (**1**; open circles) and  $\text{Cu}_2(\text{OH})_{3.04}(\text{TDC})_{0.48} \cdot 1.84\text{H}_2\text{O}$  (**3**; full triangles) compared to  $\text{Cu}_2(\text{OH})_3(\text{CH}_3\text{CO}_2) \cdot \text{H}_2\text{O}$  (open triangles).

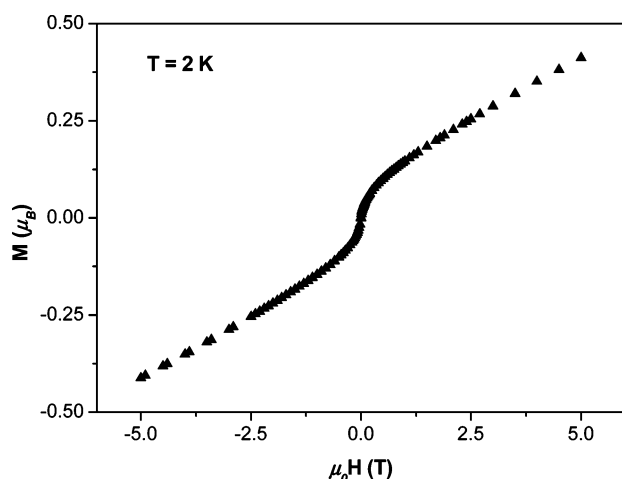


**Figure 10.** Field magnetization for  $\text{Cu}_2(\text{OH})_{3.04}(\text{TDC})_{0.48} \cdot 1.84\text{H}_2\text{O}$  (**3**) at 2 K.

regime ( $T > 200$  K) and is well-fit in this region by using the Curie–Weiss law, giving  $C = 1.02 \text{ emu} \cdot \text{K} \cdot \text{mol}^{-1}$  and  $\theta = -71.8$  K. The Curie constant is in agreement with the value for isolated Cu(II) ions, and the  $\theta$  value suggests strong antiferromagnetic interactions. There is no evidence of bulk ordering in the investigated temperature range. The Curie constant of compound **3**, equal to  $0.88 \text{ emu} \cdot \text{K} \cdot \text{mol}^{-1}$  with  $\theta = -11.7$  K, is also consistent with  $S = 1/2$  Cu(II) ions. The decrease of the  $\chi T$  product from  $0.84 \text{ emu} \cdot \text{K} \cdot \text{mol}^{-1}$  at 295 K to  $0.46 \text{ emu} \cdot \text{K} \cdot \text{mol}^{-1}$  at  $T_N = 8$  K for **3** indicates antiferromagnetic interactions. Below  $T_N$ , the abrupt rising of the  $\chi T$  product to  $0.70 \text{ emu} \cdot \text{K} \cdot \text{mol}^{-1}$  at 3 K points to a ferromagnetic-like behavior confirmed by the low-temperature magnetization versus field measurements (Figure 10). The magnetization versus field curve obtained at 2 K exhibits a sharp increase at low fields, followed by a linear and much smaller increase at higher fields. The magnetization value at 5 T ( $0.41 \mu_B$ ) is very low and far from the saturation value. This behavior is characteristic of a canted antiferromagnetic order (non-collinearity between the Cu(II) moments),<sup>63</sup> leading to weak ferromagnetism.

With regard to the hybrid compounds containing Co(II), **4** and **5**, the changes of the magnetic behavior are drastic

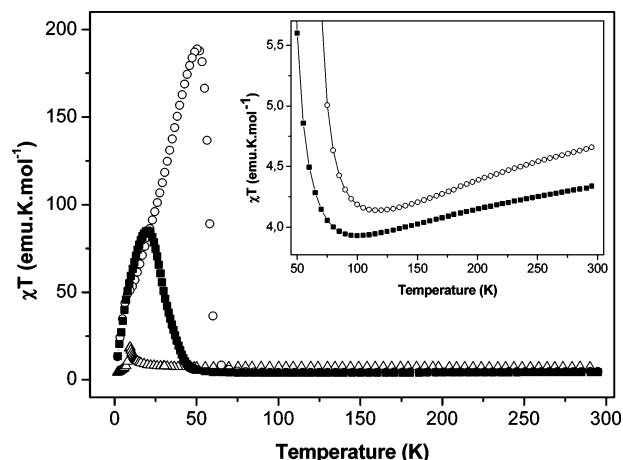


**Figure 11.** Magnetic behavior as  $\chi T$  vs  $T$  plots of the compound  $\text{Co}_2(\text{OH})_{3.38}(\text{TA})_{0.62} \cdot 1.52\text{H}_2\text{O}$  (**4**; open circles) and  $\text{Co}_2(\text{OH})_{3.44}(\text{TC})_{0.56} \cdot 0.7\text{H}_2\text{O}$  (**5**; full squares) compared to that of  $\text{Co}_2(\text{OH})_3(\text{NO}_3)$  (open triangles).

compared with that of the starting material  $\text{Co}_2(\text{OH})_3\text{NO}_3$ .<sup>53</sup> The Curie constant deduced by using the Curie–Weiss law is  $5.35 \text{ emu} \cdot \text{K} \cdot \text{mol}^{-1}$  with  $\theta = -44.3$  K for compound **4** and  $C = 4.78 \text{ emu} \cdot \text{K} \cdot \text{mol}^{-1}$  with  $\theta = -31.0$  K for compound **5**, which agrees with a mixture of tetrahedral and octahedral high spin Co(II) ions with  $C_{\text{tetra}} = 2.2$  to  $2.8 \text{ emu} \cdot \text{K} \cdot \text{mol}^{-1}$  for one Co(II) ion<sup>54,64</sup> and  $C_{\text{octa}} = 3.21 \text{ emu} \cdot \text{K} \cdot \text{mol}^{-1}$  (see also the UV data). Upon cooling, the  $\chi T$  product (Figure 11) decreases regularly from  $4.66 \text{ emu} \cdot \text{K} \cdot \text{mol}^{-1}$  at 295 K to a minimum of  $4.14 \text{ emu} \cdot \text{K} \cdot \text{mol}^{-1}$  at 115 K for the compound **4** and from  $4.34 \text{ emu} \cdot \text{K} \cdot \text{mol}^{-1}$  at 295 K to a minimum of  $3.93 \text{ emu} \cdot \text{K} \cdot \text{mol}^{-1}$  at 100 K for the compound **5**. This small decline is well-understood on the basis of a spin–orbit coupling and/or ferrimagnetic interactions between the Co(II) moments. Below 100 K, the  $\chi T$  product exhibits a continuous increase to a maximum of  $188.9 \text{ emu} \cdot \text{K} \cdot \text{mol}^{-1}$  at 50 K, followed by a decrease to  $13.2 \text{ emu} \cdot \text{K} \cdot \text{mol}^{-1}$  at 1.8 K for **4** and a maximum of  $85.0 \text{ emu} \cdot \text{K} \cdot \text{mol}^{-1}$  at 20 K, followed by a diminution to  $13.5 \text{ emu} \cdot \text{K} \cdot \text{mol}^{-1}$  at 2 K for **5**. These steep rises are related to the occurrence of long-range ferromagnetic correlations. The ordering temperatures were determined by alternating current (ac) susceptibility measurement ( $f = 30$  Hz and  $\mu_0 H_{\text{ac}} = 0.35$  mT; Figure 12). As shown in Figure 12 for  $\text{Co}_2(\text{OH})_{3.38}(\text{TA})_{0.62} \cdot 1.52\text{H}_2\text{O}$  (**4**), a sharp peak in the real part of the susceptibility  $\chi'$  is observed with a maximum at 58 K. In addition, at this temperature an abrupt onset of the imaginary part of the susceptibility,  $\chi''$ , occurs. The position of the peak in  $\chi'$  is not frequency dependent. However, two other events appear at lower temperatures, a shoulder at 19 K and a peak at 8 K. It is worth noticing that in our case the compound behaves as a hard magnet below the high-temperature transition with a strong anisotropy effect (at 40 K the coercive field is 0.29 T). It remains, however, difficult to understand which mechanism is responsible here for the low-temperature transition. These unusual features observed in the ac measurements are similar to those observed in other layered magnets, suggesting that these effects should be related to the low dimensionality of these systems.<sup>8,65</sup> The other Co(II)

(63) Kahn, O. *Molecular Magnetism*; Wiley-VCH: Weinheim, 1992; p 321.

(64) Roth, W. L. *J. Phys. Chem. Solids* **1964**, 25, 1.



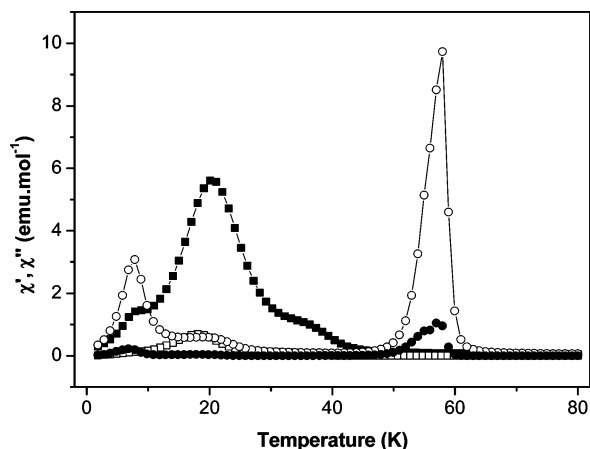


**Figure 12.** Temperature magnetic susceptibility measured in an ac field of 0.35 mT at 30 Hz for **4** ( $\chi'$ , open circles, and  $\chi''$ , full circles) and **5** ( $\chi'$ , full squares, and  $\chi''$ , open squares).

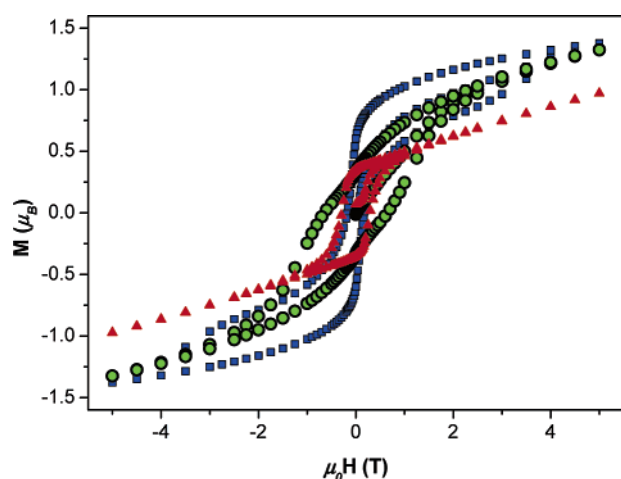


**Figure 13.** Field dependence of the magnetization of compound  $\text{Co}_2(\text{OH})_{3.38}(\text{TA})_{0.62} \cdot 1.52\text{H}_2\text{O}$  (**4**) at  $T = 1.8$  K (blue squares), at  $T = 20$  K (green circles), and at  $T = 40$  K (red triangles).

compound,  $\text{Co}_2(\text{OH})_{3.44}(\text{TC})_{0.56} \cdot 0.7\text{H}_2\text{O}$  (**5**), shows a principal peak at 20 K and two shoulders at 35 and 9 K. The ferromagnetic-type behavior of both compounds is confirmed by the presence of hysteresis loops at low temperature (Figures 13 and 14). The low value of the moments at high fields,  $M(5 \text{ T}) = 1.38$  and  $1.52 \mu_{\text{B}}$  for **4** and **5** at 1.8 K, compared to that expected for a total alignment of the moments ( $4\text{--}6 \mu_{\text{B}}$  for 2 Co(II)) suggests a ferrimagnetic order. In Figure 13, the field dependence of the magnetization of compound  $\text{Co}_2(\text{OH})_{3.38}(\text{TA})_{0.62} \cdot 1.52\text{H}_2\text{O}$  (**4**) shows hysteresis loops. At  $T = 40$  K, the coercive field is  $\mu_0 H_{\text{C}} = 0.29$  T and the magnetization  $M(5 \text{ T}) = 0.97 \mu_{\text{B}}$ , and at  $T = 20$  K, the curves indicate  $\mu_0 H_{\text{C}} = 0.65$  T and  $M(5 \text{ T}) = 1.32 \mu_{\text{B}}$  whereas at  $T = 1.8$  K, the hysteresis loop has an hourglass shape with a coercive field  $\mu_0 H_{\text{C}} = 0.18$  T which is smaller than at 20 K. According to the ac susceptibility this shape may be due to a phase transition. Because the cycle is not completely closed it may also correspond to a minor loop. The field dependence of the magnetization of compound  $\text{Co}_2(\text{OH})_{3.44}(\text{TC})_{0.56} \cdot 0.7\text{H}_2\text{O}$  (**5**), in Figure 14, shows at  $T =$

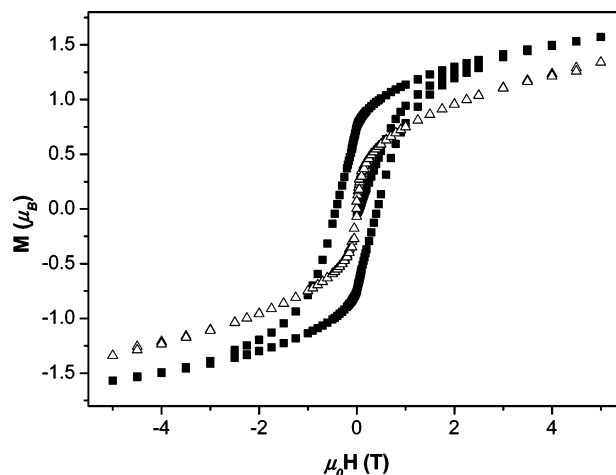


**Figure 14.** Field dependence of the magnetization of compound  $\text{Co}_2(\text{OH})_{3.44}(\text{TC})_{0.56} \cdot 0.7\text{H}_2\text{O}$  (**5**) at  $T = 1.8$  K (full circles), and at  $T = 25$  K (open triangles).

1.8 K a coercive field  $\mu_0 H_{\text{C}} = 0.43$  T and high field magnetization value  $M(5 \text{ T}) = 1.52 \mu_{\text{B}}$  whereas at  $T = 25$  K,  $\mu_0 H_{\text{C}} = 0.01$  T and  $M(5 \text{ T}) = 1.30 \mu_{\text{B}}$ . The magnetization at 1.8 K shows that the moment at 5 T is still increasing slightly but is not far from saturation. Thus the ratio of tetrahedral versus octahedral cobalt ions was roughly evaluated from the magnetization values at 5 T considering that in  $\text{Co}_2(\text{OH})_3\text{NO}_3$  (with exclusively octahedral sites)  $M_{\text{S}} = 5.74 \mu_{\text{B}}^{53}$  and by assuming that the magnetic interactions between tetrahedral and octahedral cobalt ions are antiferromagnetic. The ratios corresponding to Oh:Td sites were found to be  $\sim 62:38$  for **4** and  $\sim 63:37$  for **5**, which are in agreement with the chemical formulations (see structural part).

The studies of the magnetic properties of these hybrid materials show a drastic change from an antiferromagnetic coupling between layers for the starting compounds,  $\text{Cu}_2(\text{OH})_3(\text{CH}_3\text{CO}_2) \cdot \text{H}_2\text{O}$  and  $\text{Co}_2(\text{OH})_3\text{NO}_3$ , to ferromagnetic coupling after grafting of various thiophenecarboxylates. The physical properties of the inorganic layers are modified by the intercalation, which signifies that a cooperative phenomenon involving both the organic and the inorganic sub-networks occurs. The Cu(II) hybrid compounds containing thiopheneacetate shows antiferromagnetic behavior while the hybrid compound containing thiophenedicarboxylate exhibits a weak ferromagnetism ordering at  $T_{\text{N}} = 8$  K. The two Co(II) hydroxide-based compounds show a three-dimensional ferrimagnetic order at relatively high temperature and with high coercive fields. The compound **4**, containing the TA ligand orders at  $T_{\text{C}} = 58$  K, and the compound **5**, containing the TC ligand orders at  $T_{\text{C}} = 20$  K. Moreover, their coercive fields are  $\mu_0 H_{\text{C}} = 0.65$  T at  $T = 20$  K and  $\mu_0 H_{\text{C}} = 0.43$  T at  $T = 1.8$  K for compounds **4** and **5**, respectively. High coercive field was observed in other Co(II) parent compounds, the archetype of which is the cobalt terephthalate hydroxide.<sup>66</sup> This particular feature is currently investigated in our group in the case of Co(II) derivatives obtained with oligothiophenedicarboxylates.

(65) Bellouard, F.; Clemente-Leon, M.; Coronado, E.; Galan-Mascaros, J. R.; Gomez-Garcia, C. J.; Romero, F.; Dunbar, K. R. *Eur. J. Inorg. Chem.* **2002**, 1603.

(66) Huang, Z.-L.; Drillon, M.; Masciocchi, N.; Sironi, A.; Zhao, J.-T.; Rabu, P.; Panissod, P. *Chem. Mater.* **2000**, 12, 2805.

## Conclusions

The reaction by anionic exchange enables us to control the grafting of thiophenecarboxylate and dicarboxylates between layers of Cu(II) and Co(II) hydroxides to obtain hybrid materials. These new materials have the interest, particularly in the case of the cobalt compounds, to be ferromagnetic at relatively high temperatures with large coercive fields. However, even if the monothiophenecarboxylates show some luminescence at the solid state, no emission is observed when they are inserted between the layers. A  $\pi$ -stacking of the thiophene rings in a confined environment can be at the origin of this quenching. This work explores for the first time in this kind of compounds the possible influence of thiophene systems on the coupling between spin layers. Further development will concern the insertion of oligothiophenes with carboxylate functions, which present a better quantum yield of luminescence. These hybrid compounds should lead to the realization of multifunctional systems in which it is possible to evidence the interaction between magnetization and photoluminescence or photoconduction.

## Experimental Section

**General Remarks.** The powder XRD patterns were collected with a Siemens D 500 diffractometer (Co  $K\alpha_1 = 1.788\ 97\ \text{\AA}$ ) for the cobalt(II) products and with a Siemens D 5000 diffractometer (Cu  $K\alpha_1 = 1.540\ 598\ \text{\AA}$ ) in the case of the copper compounds. FT-IR studies were carried out with an ATI Mattson Genesis computer-driven instrument. UV/vis/near-infrared studies were performed on a Perkin-Elmer Lambda 19 instrument (spectra recorded by reflection with a resolution of 4 nm and a sampling rate of  $240\ \text{nm}\cdot\text{min}^{-1}$ ). TGA experiments were performed on a Setaram TG 92 instrument (heating in air from 20 to  $900\ ^\circ\text{C}$  at a rate of 0.5, 2, or  $5\ ^\circ\text{C}\cdot\text{min}^{-1}$ ). Elemental analyses for C, H, and S were carried out by the Analytical Department at the Institut Charles Sadron (Strasbourg, France). The Cu and Co metal contents were determined by inductively coupled plasma mass spectroscopy on samples dissolved in  $\text{HNO}_3$  by the Analytical Department of the Ecole de Chimie, Polymères, Matériaux de Strasbourg. SEM observations were made with a JEOL JSM-840 instrument. Magnetic data were collected with a SQUID magnetometer (Quantum Design MPMS-XL) covering the temperature and field ranges 2–300 K,  $\pm 5\ \text{T}$ . ac susceptibility measurements were performed in a 0.35 mT alternative field (30 Hz). Thiophenecarboxylic acids (Aldrich, 99%),  $\text{CoCl}_2\cdot 6\text{H}_2\text{O}$  (Aldrich, 99%), were used as purchased.  $\text{Cu}_2(\text{OH})_3(\text{CH}_3\text{CO}_2)\cdot\text{H}_2\text{O}^{36}$  and  $\text{Co}_2(\text{OH})_3(\text{NO}_3)^{53}$  were prepared as previously described. All experiments were conducted under argon, and the solvents were degassed prior to use. Note that the number of grafted thiophenecarboxylates is very dependent on the experimental conditions. Thus slight differences in temperature or duration of the treatment can lead to compounds with not exactly the same composition. The range of insertion per two metallic atoms was observed to be between 0.5 and 0.9 for one carboxylate function. In this range the XRD patterns and magnetic behaviors are unchanged.

**$\text{Cu}_2(\text{OH})_{3.28}(\text{C}_4\text{H}_3\text{SCH}_2\text{CO}_2)_{0.72}\cdot 0.08\text{H}_2\text{O}$  (1).** An aqueous solution of 0.2 M NaOH was added dropwise to a solution of 3-thiopheneacetic acid (0.71 g; 5 mmol) in 15 mL of water. At pH 8.3,  $\text{Cu}_2(\text{OH})_3(\text{CH}_3\text{CO}_2)\cdot\text{H}_2\text{O}$  (0.25 g; 1 mmol) was added, and the suspension was stirred for 24 h at room temperature. After filtration and washing with water and ethanol, the precipitate was dispersed

in 20 mL of water for 14 h at room temperature. Then the green powder was filtered off and washed with water and ethanol (yield > 70% on the basis of  $\text{Cu}_2(\text{OH})_3(\text{CH}_3\text{CO}_2)\cdot\text{H}_2\text{O}$ ).

Anal. Calcd (%) for  $\text{C}_{4.32}\text{H}_{7.04}\text{S}_{0.72}\text{O}_{4.80}\text{Cu}_2$  ( $M_w = 280.56\ \text{g}$ ): C, 18.49; H, 2.53; S, 8.23. Found: C, 18.50; H, 2.78; S, 8.01. Copper %: calcd, 45.3; found, 45.3. IR (KBr pellet,  $\text{cm}^{-1}$ ): 3430 sh ( $\nu(\text{OH}-\text{O})$ ), 3100 w ( $\nu(\text{CH})$ ), 2925 w ( $\nu(\text{CH}_2)$ ), 1555 vs ( $\nu_{\text{as}}(\text{C}=\text{O})$ ), 1385 vs ( $\nu_s(\text{C}-\text{O})$ ), 1275 s, 1155 w, 1085 w, 920 w, 835 s ( $\delta_{\text{oop}}(\text{CH})$ ), 740 s ( $\delta_{\text{oop}}(\text{CH})$ ), 690 s ( $\delta_{\text{oop}}(\text{CH})$ ), 615 s. UV-vis (diffuse reflectance): 250 and 685 nm

**Attempted Preparation of  $\text{Cu}_2(\text{OH})_{3.32}(\text{C}_4\text{H}_3\text{SCO}_2)_{0.68}\cdot 0.1\text{H}_2\text{O}$  (2).** An aqueous solution of 0.2 M NaOH was added dropwise to a solution of 2-thiophenecarboxylic acid (0.65 g; 5 mmol) in 15 mL of water. At pH 9.1,  $\text{Cu}_2(\text{OH})_3(\text{CH}_3\text{CO}_2)\cdot\text{H}_2\text{O}$  (0.25 g; 1 mmol) was added, and the suspension was stirred during 24 h at room temperature. After filtration and washing with water and ethanol, the precipitate was dispersed in 20 mL of water for 20 h at room temperature. Then the brown powder was filtered off and washed with water and ethanol.

Anal. Found (%): C, 17.30; H, 1.73; S, 9.50. Copper %: found, 45.1. IR (KBr pellet,  $\text{cm}^{-1}$ ): 3570 w ( $\nu(\text{OH})$ ), 3435 sh ( $\nu(\text{OH}-\text{O})$ ), 1575 vs ( $\nu_{\text{as}}(\text{C}=\text{O})$ ), 1425 vs ( $\nu(\text{C}=\text{C})$ ), 1375 vs ( $\nu_s(\text{C}-\text{O})$ ), 1340 s ( $\nu(\text{C}=\text{C})$ ), 1230 w, 1120 w, 1035 w, 900 s, 765 s, 705 s. UV-vis (diffuse reflectance): 255 and 700 nm. The desired product could not be isolated cleanly, and no satisfactory elemental analysis could be obtained because of unidentified impurities.

**$\text{Cu}_2(\text{OH})_{3.04}(\text{C}_4\text{H}_2\text{SC}_2\text{O}_4)_{0.48}\cdot 1.84\text{H}_2\text{O}$  (3).** An aqueous solution of 0.2 M NaOH was added dropwise to a solution of 2,5-thiophenedicarboxylic acid (0.34 g; 2 mmol) in 15 mL of water. At pH 10.5,  $\text{Cu}_2(\text{OH})_3(\text{CH}_3\text{CO}_2)\cdot\text{H}_2\text{O}$  (0.25 g; 1 mmol) was added, and the suspension was stirred during 24 h at room temperature. After filtration and washing with water and ethanol, the precipitate was redispersed in 20 mL of water for 20 h at room temperature. Then the green powder was filtered off and washed with water and ethanol (yield > 70% on the basis of  $\text{Cu}_2(\text{OH})_3(\text{CH}_3\text{CO}_2)\cdot\text{H}_2\text{O}$ ).

Anal. Calcd (%) for  $\text{C}_{2.88}\text{H}_{7.68}\text{S}_{0.48}\text{O}_{6.80}\text{Cu}_2$  ( $M_w = 293.62\ \text{g}$ ): C, 11.78; H, 2.64; S, 5.24. Found: C, 11.58; H, 2.43; S, 5.26. Copper %: calcd, 43.3; found, 43.3. IR (KBr pellet,  $\text{cm}^{-1}$ ): 3370 sh ( $\nu(\text{OH}-\text{O})$ ), 1545 vs ( $\nu_{\text{as}}(\text{C}=\text{O})$ ), 1460 w ( $\nu(\text{C}=\text{C})$ ), 1370 ( $\nu_s(\text{C}-\text{O})$ ), 1310 w, 1240 w, 1155 w, 1090 w, 1015 w, 930 s, 765 s, 680 s. UV-vis (diffuse reflectance): 265 and 650 nm.

**$\text{Co}_2(\text{OH})_{3.38}(\text{C}_4\text{H}_3\text{SCH}_2\text{CO}_2)_{0.62}\cdot 1.52\text{H}_2\text{O}$  (4).** An aqueous solution of 0.2 M NaOH was added dropwise to a solution of 3-thiopheneacetic acid (0.71 g; 5 mmol) in 15 mL of water. At pH 8.0,  $\text{Co}_2(\text{OH})_3(\text{NO}_3)$  (0.23 g; 1 mmol) was added, and the suspension was stirred for 23 h at  $50\ ^\circ\text{C}$ . The blue crystalline powder was filtered off and washed with water and ethanol (yield > 70% on the basis of  $\text{Co}_2(\text{OH})_3(\text{NO}_3)$ ).

Anal. Calcd (%) for  $\text{C}_{3.72}\text{H}_{9.52}\text{S}_{0.62}\text{O}_{6.14}\text{Co}_2$  ( $M_w = 290.3\ \text{g}$ ): C, 15.39; H, 3.31; S, 6.85. Found: C, 15.38; H, 3.01; S, 6.67. Cobalt %: calcd, 40.6; found, 40.6. IR (KBr pellet,  $\text{cm}^{-1}$ ): 3570 w ( $\nu(\text{OH})$ ), 3455 b ( $\nu(\text{OH}-\text{O})$ ), 3100 w ( $\nu(\text{CH})$ ), 2920 w ( $\nu(\text{CH}_2)$ ), 1655 w ( $\delta(\text{H}_2\text{O})$ ), 1545 vs ( $\nu_{\text{as}}(\text{C}=\text{O})$ ), 1385 vs ( $\nu_s(\text{C}-\text{O})$ ), 1280 s, 1020 s, 835 s ( $\delta_{\text{oop}}(\text{CH})$ ), 740 s ( $\delta_{\text{oop}}(\text{CH})$ ), 700 s ( $\delta_{\text{oop}}(\text{CH})$ ). UV/vis (diffuse reflectance) for octahedral coordination of Co(II),  $\lambda = 1274\ (^4\text{T}_{1g} \rightarrow ^4\text{T}_{2g})$ , 600 ( $^4\text{T}_{1g} \rightarrow ^4\text{A}_{2g}$ ), 500 nm ( $^4\text{T}_{1g} \rightarrow ^4\text{T}_{1g}(\text{P})$ ); for tetrahedral coordination of Co(II),  $\lambda = 1538\ (^4\text{A}_2 \rightarrow ^4\text{T}_1(\text{P}))$ , 615 nm ( $^4\text{A}_2 \rightarrow ^4\text{T}_1(\text{P})$ ).

**$\text{Co}_2(\text{OH})_{3.44}(\text{C}_4\text{H}_3\text{SCO}_2)_{0.56}\cdot 0.7\text{H}_2\text{O}$  (5).** An aqueous solution of 0.2 M NaOH was added dropwise to a solution of 2-thiophenecarboxylic acid (0.64 g; 5 mmol) in 15 mL of water. At pH 8.2,  $\text{Co}_2(\text{OH})_3(\text{NO}_3)$  (0.23 g; 1 mmol) was added, and the suspension was stirred during 22 h at  $50\ ^\circ\text{C}$ . The blue crystalline powder was filtered

off and washed with water and ethanol (yield > 70% on the basis of  $\text{Co}_2(\text{OH})_3(\text{NO}_3)$ ).

Anal. Calcd (%) for  $\text{C}_{2.8}\text{H}_{6.52}\text{S}_{0.56}\text{O}_{5.26}\text{Co}_2$  ( $M_w = 260.2$  g): C, 12.93; H, 2.53; S, 6.90. Found: C, 12.89; H, 2.74; S, 6.99. Cobalt %: calcd, 45.3; found, 45.3. IR (KBr pellet,  $\text{cm}^{-1}$ ): 3415 sh ( $\nu(\text{OH}-\text{O})$ ), 1555 vs ( $\nu_{\text{as}}(\text{C}=\text{O})$ ), 1425 vs ( $\nu(\text{C}=\text{C})$ ), 1385 vs ( $\nu_{\text{s}}(\text{C}-\text{O})$ ), 1340 s ( $\nu(\text{C}=\text{C})$ ), 1225 w, 1115 w, 1035 w, 860 s, 800 s, 775 s, 715 s, 660 s. UV/vis (diffuse reflectance) for octahedral coordination of Co(II),  $\lambda = 1225$  ( $^4\text{T}_{1\text{g}} \rightarrow ^4\text{T}_{2\text{g}}$ ), 600 ( $^4\text{T}_{1\text{g}} \rightarrow ^4\text{A}_{2\text{g}}$ ), 495 nm ( $^4\text{T}_{1\text{g}} \rightarrow ^4\text{T}_{1\text{g}}(\text{P})$ ); for tetrahedral coordination of Co(II),  $\lambda = 1565$  ( $^4\text{A}_2 \rightarrow ^4\text{T}_1(\text{F})$ ), 620 nm ( $^4\text{A}_2 \rightarrow ^4\text{T}_1(\text{P})$ ).

**Acknowledgment.** We thank D. Burger for the ATG measurements, A. Derory for the magnetic measurements, and C. Leuvrey for SEM images. This work was supported by the CNRS, the Université Louis Pasteur de Strasbourg, and the European Community (European Network of Excellence MAG-MANet, Sixth Framework programme – Priority [3-NMP], Proposal/Contract No. 515767-2). A.D. thanks the French Ministry for Education Research and Technology for her Ph.D. grant.

CM060366W